http://dx.doi.org/10.5012/bkcs.2012.33.3.848

Computational Study on Oligomer Formation of Fibril-forming Peptide of α-Synuclein†

SeongByeong Park, Jeseong Yoon, Soonmin Jang,‡ Kyunghee Lee,‡ and Seokmin Shin*

*School of Chemistry, Seoul National University, Seoul 151-747, Korea. *E-mail: sshin@snu.ac.kr*
‡Department of Chemistry, Sejong University, Seoul 143-747, Korea
Received December 16, 2011, Accepted December 30, 2011

We have studied the oligomerization of a fibril-forming segment of α-Synulcein using a replica exchange molecular dynamics (REMD) simulation. The simulation was performed with trimers and tetramers of a 12 amino acid residue stretch (residues 71-82) of α-Synulcein. From extensive REMD simulations, we observed the spontaneous formation of both trimer and tetramer, demonstrating the self-aggregating and fibril-forming properties of the peptides. Secondary structure profile and clustering analysis illustrated that antiparallel β-sheet structures are major species corresponding to the global free energy minimum. As the size of the oligomer increases from a dimer to a tetramer, conformational stability is increased. We examined the evolution of simple order parameters and their free energy profiles to identify the process of aggregation. It was found that the degree of aggregation increased as time passed. Tetramer formation was slower than trimer formation and a transition in order parameters was observed, indicating the full development of tetramer conformation which is more stable than that of the trimer. The shape of free energy surface and change of order parameter distributions indicate that the oligomer formation follows a dock-and-lock process.

Key Words : α-Synuclein, Replica-exchange molecular dynamics (REMD), Fibril formation, Antiparallel β-sheet

Introduction

In many neurodegenerative diseases including Alzheimer's, Creutzfeldt-Jacob, and Parkinson's disease, deposits of aggregated proteins are found at the neuronal surface in the form of amyloid-like fibrils.[1,2] The pathologies of these diseases, especially the mechanism of formation of oligomers or fibrils have been great interest and the subject of extensive experimental research.[3-5] Numerous biophysical and biochemical experimental studies have made substantial advances and revealed some common features such as cross-β X-ray diffraction patterns.[6,7] Regardless of these advances, detailed information on the structures and formation mechanism of protein aggregates at atomistic levels, and also the interpretation of experimentally revealed structural features based on atomic level studies, are rather limited. For example, we do not yet have clear explanations for the following questions: what molecular features give rise to cross-β spine structure?; Do amyloid proteins have native structures?; Is the amyloid-like fibril formation from a general peptide backbone structure or is it sequence specific?.[6] Limitations in structural studies through experiments on these proteins have partly arisen from the non-crystalline and insoluble nature of amyloid fibrils. More importantly, corresponding proteins are intrinsically unstructured and exhibit noticeable conformational plasticity, which is highly sensitive to environmental conditions.[8] The characteristics of the so-called "intrinsically unstructured or "intrinsically disordered proteins have been actively investigated in recent years.[9-11] It has been gradually recognized that the study of unfolded or partially folded states of natively or intrinsically unstructured proteins is essential to the understanding of some biological processes. In fact, numerous proteins lacking an intrinsic globular structure under physiological condition have been recognized and many of them are found to be involved in important regulatory functions inside cells. Such inherent flexibility of those proteins is supposed to acts as a functional advantage in such a way that they can bind multiple targets, depending on cell conditions. Rapid turnover in the solution state facilitates the sensitivity of the cell cycle to external conditions.

A number of recent observations has provided substantial evidence that aggregation of α-Synulcein is a critical step in the pathogenesis of Parkin's disease (PD).[12] In particular, the fibril formed from α-Synulcein is the primary component of Lewy bodies (LBs) and Lewy neurites (LNs) that are the diagnostic hallmarks of PD.[13-15] α-Synulcein is a 140 residue protein primarily found in neural tissue, especially in presynaptic terminals. It has been suggested that α-Synulcein plays an important role in the pathogenesis of several neurodegenerative disorders. Circular dichroism (CD) or other optical experimental methods have shown that α-Synulcein does not appear to possess a well-defined native structure, indicating its intrinsically unstructured nature.[16,17] α-Synulcein also exhibits a remarkable conformational plasticity depending on its environmental conditions[18]. The flexible structure of α-Synulcein makes it versatile in its

†This paper is to commemorate Professor Kook Joe Shin's honourable retirement.

interaction with other proteins.[19] α-Synulcein was shown to adopt a mostly helical secondary structure upon association with small unilamellar vesicles or detergent micelle surfaces.[20] It is reported that the region referred to as the non-amyloid component (NAC), corresponding to a 61-95 amino acid sequence of human α-Synulcein, plays a crucial role in fibril formation.[21]

Due to a remarkable increase in computational resources as well as developments in computational algorithms, one of the most direct and prominent theoretical approaches to investigate the structures and dynamics of protein misfolding aggregation at the molecular level is to perform systematic molecular dynamics simulations.[22] Computational studies form an integral part of multidisciplinary approaches to elucidating various amyloid assemblies.[23]

Recent experimental results suggest that a hydrophobic stretch of 12 amino acid residues in the middle of the NAC region is essential for filament assembly; also noted is that this 12 residue sequence of peptides can self-aggregate and form a fibril showing a β-sheet like CD spectrum.[24] The same region was predicted to be "aggregation-susceptible with a high intrinsic propensity for aggregation.[25] In our previous work, we have performed replica-exchange molecular dynamics simulations on a pair of peptides corresponding to the 71-82 sequence in α-Synulcein to investigate the dimerization process and the structural features of a conformational ensemble of dimeric aggregates.[26,27]

In this paper, we have extended our previous work in order to study the aggregation processes and structural features of the trimer and tetramer. We have performed extensive REMD simulations to investigate the self-aggregation process of the peptides. All-atom protein force field and implicit generalized-Born/surface area solvent models have been employed. We examined the evolution of simple order parameters and their free energy profiles to identify the process of aggregation and compare the differences in processes between trimer and tetramer formation. This work supports experimentally reported self-aggregating properties of the 71-82 sequence in α-Synulcein. It is important to elucidate the role of oligomer formation in the pathway of fibrillization of α-Synulcein. The results of the present study are expected to provide useful information on the oligomer formation processes of hydrophobic peptides.

Model and Simulation Details

Oligomerization process of a peptide involves orientational rearrangement and conformational change. One needs to use computational schemes based on efficient conformational sampling or relevant conformational constraints in order to describe such an aggregation process in a reasonable computation time. REMD simulation has been performed as an efficient sampling scheme for processes involving complex biomolecules.[28] In an attempt to observe the spontaneous ordering of oligomers, we have performed replica exchange molecular dynamics (REMD) simulation for fibril-forming peptides of α-Synulcein. To perform the simulation process, a linear chain of α-Synulcein (71-82) sequence (VTGVTAV AQKTV) is prepared and copied to build trimers and tetramers. Initially, each peptide is randomly placed inside the simulation box. Peptides are confined within an imaginary sphere such that if the atoms are beyond the given boundary distance from the center of mass of the system, the attracting harmonic force centered at that boundary position will prohibit the molecules from flying apart from each other. The radius was chosen to be 30 Å for trimers and 38 Å for tetramers, which are found to allow each peptide to move freely inside the sphere without severely disturbing the motion of the other peptide. After this minimization process, the system is heated up to 500 K for 300 ps in order to obtain initial coordinates with randomly distributed conformations. At the next step, normal molecular dynamics simulation is performed for 500 ps on each replica without exchange, to equilibrate each replica at each corresponding temperature. The number of replicas for REMD simulation is 16 for trimers, and 24 for tetramers. The temperature distribution of REMD for trimer simulation includes 290, 300, 310.7, 322.1, 334.2, 347, 360.5, 374.7, 389.6, 405.2, 421.5, 438.5, 456.2, 474.6, 493.7, and 513.5 K. For tetramer simulation, the temperature distribution includes 290, 294.5, 299.9, 306.2, 313.4, 321.5, 330.5, 340.4, 351.2, 362.9, 375.5, 389, 403.4, 418.7, 434.9, 452, 470, 488.9, 508.7, 529.4, 551, 573.5, 596.9, 621.2 K. The exchange interval is every 200 steps (0.4 ps) and coordinates are recorded every 0.4 ps for further analysis. The exchange ratio is found to be > 20% for trimer simulation and 30-40% for tetramer simulation. Simulations have been carried out using AMBER.[29] We used an AMBER parm96 force field with an implicit solvation model by Onufriev, Bashford, and Case.[30] This solvation model is a modified Generalized-Born model in which the effective Born radii are re-scaled to account for the interstitial spaces between atom spheres missed in previous model, being intended to be a closer approximation to the true molecular volume. This combination was shown to be the most consistent in capturing the behavior of various peptides, maintaining a balance between strand and helical conformations.[31] Periodic boundary conditions were used and the cut-off distance was 20 Å. The SHAKE[32] algorithm was used for bond constraints and the time step was 2 fs for all simulations. Total REMD simulation time is 360 ns for trimer simulation and 500 ns for tetramer simulation. Secondary structure contents, radius of gyrations, clustering analysis, and principle component calculations are carried out using analysis modules in AMBER. In addition, we have introduced simple order parameters $P=\frac{1}{nL}\Sigma_{i=1}^{n}\|\vec{r}_I\|$ and $Q=\frac{1}{nC2}\Sigma_{i<j}^{n-1}|\langle \vec{u}_I, \vec{u}_J\rangle|$, to examine the process of aggregation, where $\vec{r}_I$ is an end-to-end vector between N-terminal and C-terminal alpha carbons of the *i*-th peptide, *n* is the number of peptides, $L=\max(\|\vec{r}_I\|)$, and $\vec{u}_I=\frac{\vec{r}_I}{\|\vec{r}_I\|}$. Here, *P* measures average end-to-end distance of a single peptide stretch in an oligomer and *Q* measures the average degree of alignment between every pair of peptides. If all peptides are in an extended conformation, *P* is close to 1, and for the opposite case, *P* is small. If all peptides are well aligned as a

beta sheet conformation, Q is close to 1, and for poorly aligned conformations, Q will be small. Therefore, we expect that we can trace the change of conformations by monitoring the time evolution of P and Q values. All the results presented have been obtained from 300K data.

Results and Discussion

REMD simulations of trimer and tetramer formation have been performed using the REMD parameters, temperature distributions and force field with implicit solvation model described in the method section. To measure the degree of convergence, principle component (PC) analysis was done and the first two major principle component vectors were calculated. A PC space convergence test[33] shows pseudo-convergence from about 80ns with a small degree of slope for trimers (Fig. 1(a)). The convergence is much faster than that for the dimer simulation.[26] A comparison of the secondary structure evolution pattern of dimer aggregation with trimer aggregation implies that the slower convergence in dimer aggregation might be due to the large contribution of various monomeric conformational states during the time evolution, whereas the contributions of monomeric states and dimer-monomer states are relatively small for trimer aggregation. For tetramers, pseudo-convergence of the trajectory in PC space occurs around 160 ns (Fig. 1(b)). The convergence for the tetramer is slower than that for the trimer simulation and is comparable to that for the dimer case.[26] By examining the time evolutions of radius of gyration and secondary structure contents (Fig. 2), it can be argued that the slower convergence is mainly due to longer time scales for building tetrameric conformations. Unlike natively folded single chain proteins, oligomeric system composed of a small number of peptides with a chain length of a dozen amino acid residues, may not posess the most thermodynamically stable single energy minimum conformations. Rather, it may be essentially a "dynamical system" composed of various conformational states which are interconnected by frequent conformational transformations. This behavior is illustrated in the time evolution patterns of radius of gyration and secondary structure contents (Fig. 2).

As with dimer formation, we observed the self-aggregation of trimers and tetramers. Antiparallel beta sheet conformations are identified as the dominant species. From the secondary structure and radius of gyration profiles (Fig. 2), one can estimate the time scale for full oligomer formation. For dimers, the highest anti parallel beta sheet content and the lowest radius of gyration occur near 10 ns, indicating the first full dimer formation at this time.[26] Similarly, trimer formation occurs around 30 ns, while full tetramer formation requires much longer time of about 150 ns. The order of time scales for oligomer formation is dimer < trimer < tetramer. On the other hand, degrees of fluctuation on beta sheet content and radius of gyration indicate that the conformational stabilities are proportional to the oligomer formation time: dimers are easily formed but rather unstable, trimers are a less easily formed species than dimer but stay stable much longer than dimers, and tetramers show greater stability compared to dimers and trimers, even though they are not easily formed.

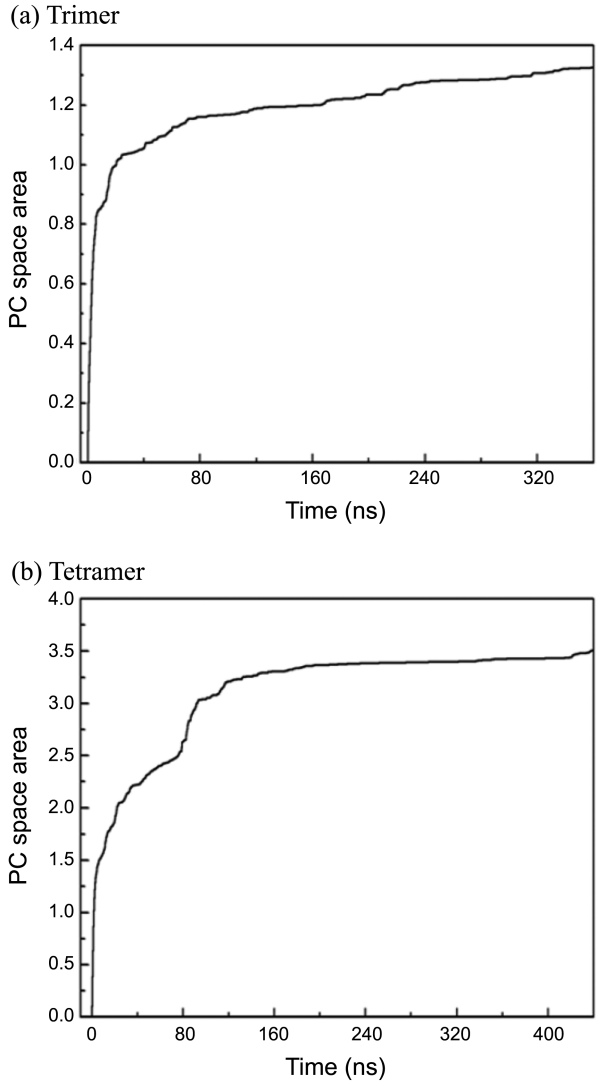

Figure 1. Time evolutions of the areas in PC space covered by simulation trajectories of (a) trimer and (b) tetramer simulations for residues 71-82 of a-Synuclein with the AMBER parm99SB force field. Vertical axis is the visited PC space area ($\times 10^4$ Å).

To examine the diversity of conformational ensembles more closely, we have performed clustering analysis on the last 100 ns of data of the whole simulation trajectory. The results are shown in Figure 3 and Figure 4. Clustering analysis results identify two features. For trimer simulation, it shows no noticeable monomer conformations, and trimer conformations dominate with a small contribution of monomer-dimer conformations. Figure 3 clearly shows that every dimer and trimer structure adopts antiparallel β-sheet conformation, and the major conformation is a trimeric antiparallel β-sheet. Similarly, clustering analysis on tetramer simulation trajectory also shows that anti parallel tetrameric beta sheet conformations are the dominant species, with a small contribution of trimer-monomer and dimer-dimer species (Fig. 4). This result is consistent with dimer simulation, and

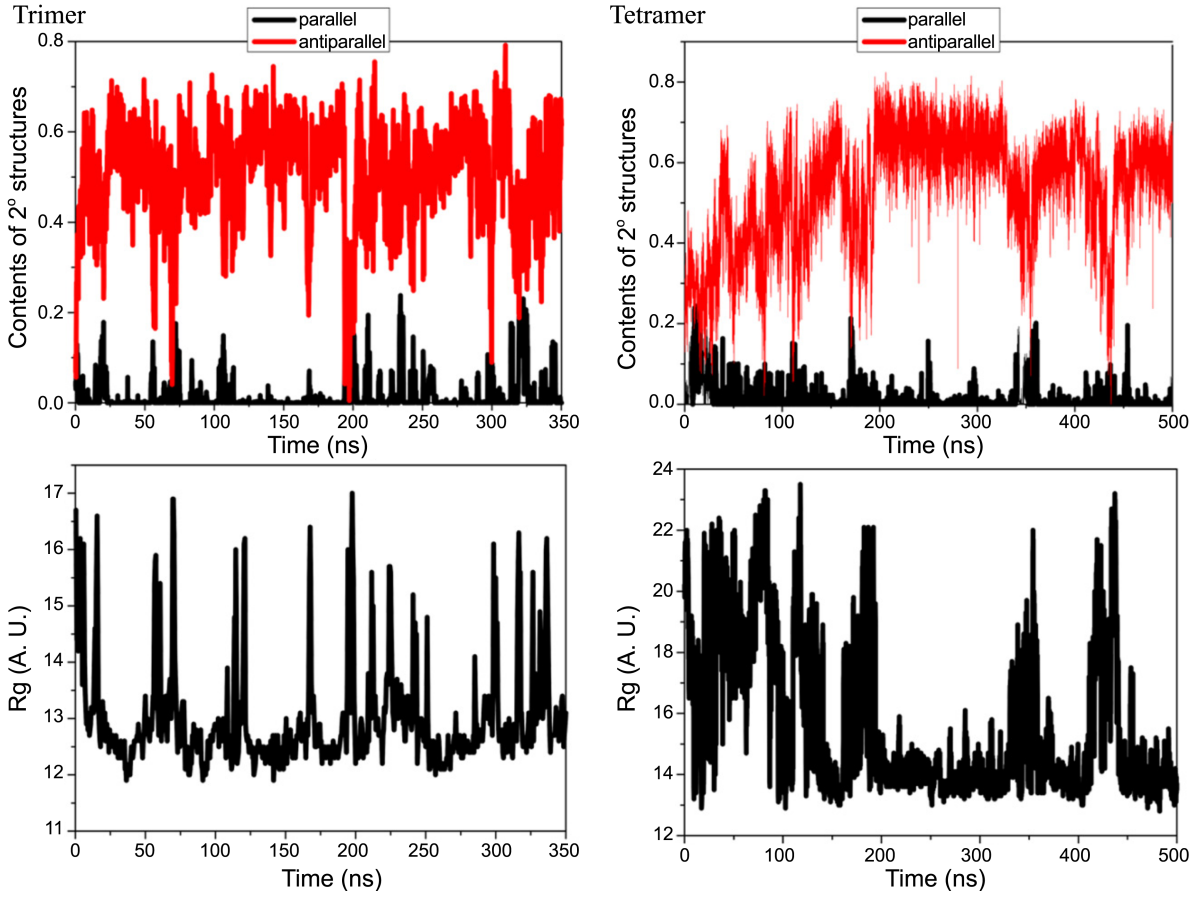

Figure 2. Time evolutions of the secondary structure contents and radius of gyrations from simulation trajectories of trimer and tetramer simulations.

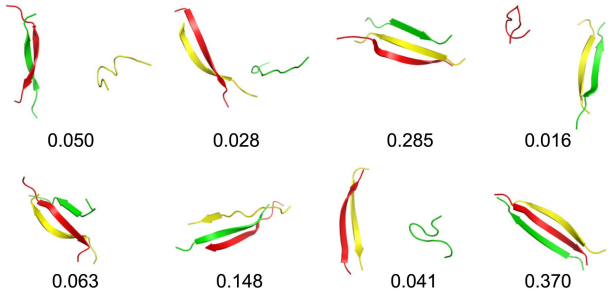

Figure 3. Eight major trimer conformers obtained by clustering analysis from simulation trajectories of trimer simulations.

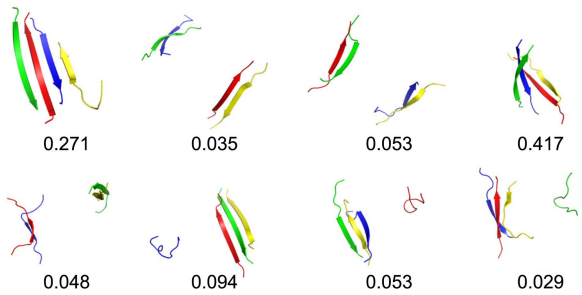

Figure 4. Eight major tetramer conformers obtained by clustering analysis from simulation trajectories of tetramer simulations.

further, consistent with the explicit water simulation results in our previous work.[26] In trimer simulations, trimeric species occupies almost 90% of whole conformations. On the other hand, in tetramer simulations, tetrameric species occupy only 72%, with ~18% of trimeric species. It can be argued that the trimer to tetramer transition barrier is higher than the dimer to trimer barrier.

We examined free energy surfaces using radius of gyration and anti parallel beta sheet content as two order parameters (Fig. 5). The free energy was calculated using the trajectory at room temperature (300 K). These free energy surfaces show two features. First, trimer formation has no noticeable free energy barrier, whereas tetramer formation has a sharp barrier with a barrier height of ~1.2 kcal/mol. This is comparable to a hydrogen bond energy forming beta sheet. The trimer barrier height is ~0.3 kcal/mol which is smaller than thermal energy at 295 K. Secondly, both free energy surfaces have L-shape topology, which implies that the formation of oligomers occurs in a dock-and-lock fashion.[34]

To examine this dock-and-lock feature in close detail, we defined two simple order parameters, P and Q, representing degrees of linearity and alignment, respectively. The change of distribution of P in time showed that trimeric species form at an early stage as a dominant species while tetramers exhibit gradual formation. The time evolution of distribution for P also suggests a transition from trimer-monomer

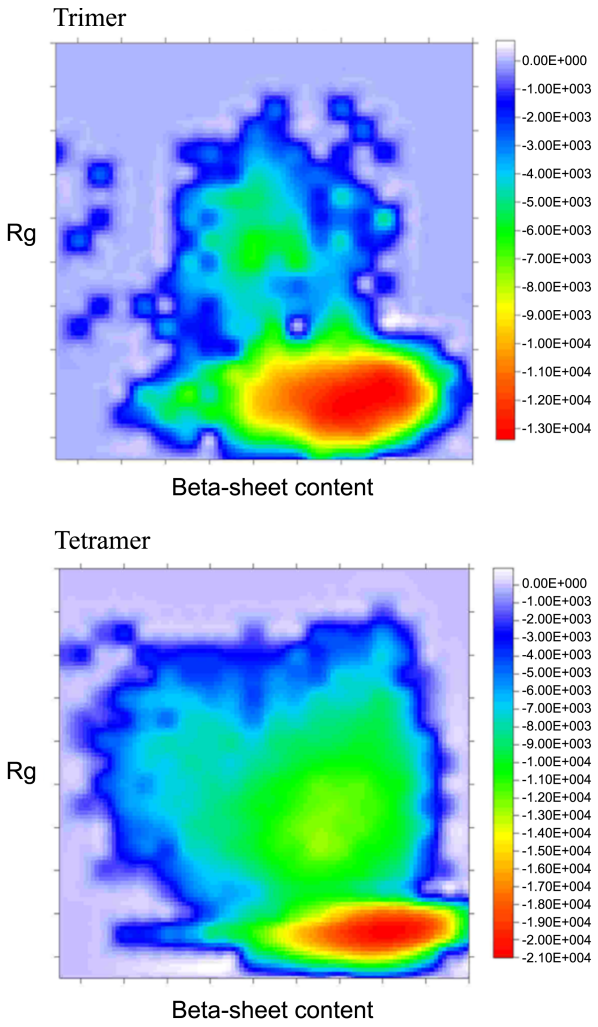

Figure 5. Free energy surface as a function of radius of gyration and anti parallel beta sheet content obtained from the trajectories of trimer and tetramer simulations.

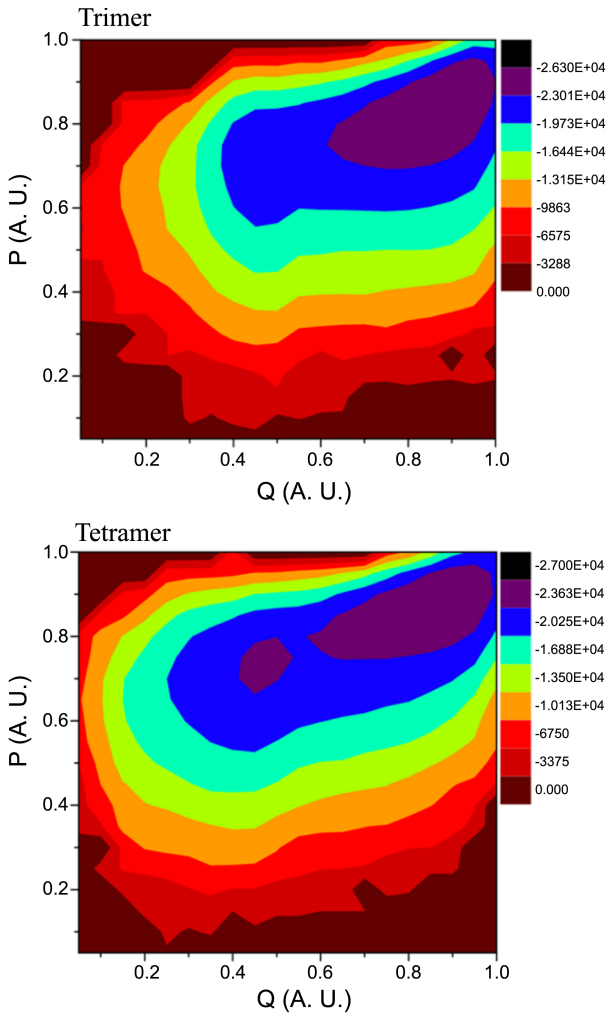

Figure 6. Free energy surface as a function of order parameters P and Q obtained from the trajectories of trimer and tetramer simulations.

conformations to tetrameric conformations. Such transition is not apparent in trimer distribution because the equilibrium between dimeric and trimeric species is quickly achieved. The distribution for Q also demonstrates these differences. The Q distribution for trimers has two distinct peaks and this distribution does not show a noticeable change in time, indicating that dimer-trimer equilibration is achieved from the early stage and doesn't change in time. On the contrary, tetramer simulation reveals a dramatic change of Q distribution in time, illustrating that dimeric and trimeric species disappear gradually and transform to tetrameric species. Consequently, the time evolutions of P, Q distributions suggest that the trimer formation process has no transition barrier, whereas the tetramer formation process has a transition barrier.

We have also examined the free energy surfaces in (P, Q) space (Fig. 6). The overall shape of free energy surfaces for both trimer and tetramer show an L-shape topology, which means that the aggregation processes generally follow a dock-and-lock fashion even for the peptide molecules of very short chain length like these. Figure 6 shows that trimer formation has no barrier and tetramer formation has a transition barrier. Examining the change of free energy surface in a discrete time interval shows this difference more clearly: for trimers, the location of an energy minimum basin does not change with time. For tetramers, the location of an energy minimum basin moves from the low (P, Q) region to high (P, Q) region, corresponding to dimer-dimer and tetramer conformations, respectively.

To further investigate this barrier transition behavior, we have revisited the secondary structure content and radius of gyration profile by examining change of distribution in time. The distributions of secondary structure profile and radius of gyration for trimers do not show large changes in time, illustrating fast aggregation into trimeric conformations. The time dependence of the beta sheet content distribution implies that full beta sheet hydrogen bonds between peptide backbones require slightly more time than aggregation, which is consistent with a dock-and-lock aggregation mechanism. The distribution for tetramers shows clear pattern of change in time. The sharp peak near smaller R_g increases rapidly while the broad peak near larger R_g decreases, indicating the gradual formation of compact tetrameric species with a

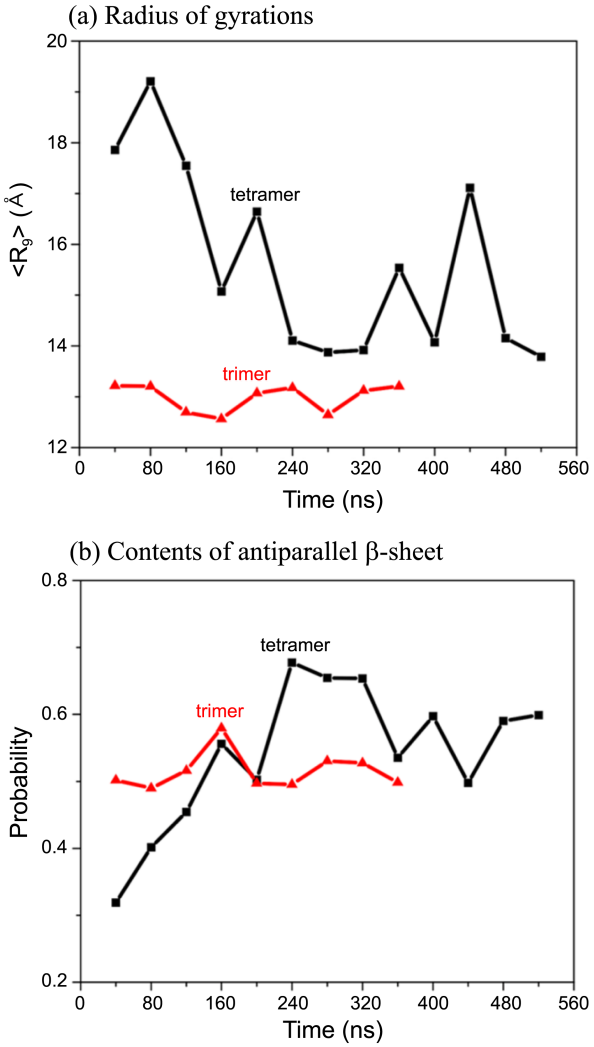

Figure 7. Time evolutions of (a) radius of gyrations and (b) contents of antiparallel b-sheet for different time periods obtained from the trajectories of trimer and tetramer simulations.

decreasing population of dimer-dimer and trimer-mononer species. Anti parallel beta sheet content also shows a transition of the major peak toward larger values, clearly showing the formation of antiparallel beta sheet tetramer conformations. It is noted that the change of minimum energy basin in (*P*, *Q*) free energy surface is due to the formation of high beta sheet content conformations (tetramer species). Figure 7 shows the time evolution of average values for radius of gyration and beta sheet content. The decrease of beta sheet content around 200 ns in Figure 7 can be understood as the transient relaxation of backbone hydrogen bonds in a trimer beta sheet in order to adopt an additional monomer in order to form a tetramer. The sudden increase of radius of gyration at the same time supports this picture. It can be deduced that the tetramer beta sheet formation process has a noticeable free energy barrier because the transition state should have less compact trimeric conformation with relaxed hydrogen bonding between backbone atoms in order to accept additional monomer unit.

From the experimental and computational studies on peptide aggregation processes, several distinct scenarios have been suggested. The two step dock-lock-mechanism suggests that the partially structured collapsed state of monomer is added first by a diffusion-limited process, and subsequently undergoes reorganization of structures to form oligomer conformations. On the other hand, the one step mechanism proposes the aggregation-prone state achieved by conformational fluctuations, which then derives the proto-fibril state. Thirumalai *et al.*[35] have suggested the general unified picture, in which partial unfolding or partial folding produce an aggregation-prone state, and this state accelerates the formation of a critical nucleus. The next step is the growth of oligomers by dock-and-lock style monomer addition. Despite the short length of our peptides, they would prefer energetically the most stable oligomeric conformation. The monomer conformation in this state can be considered as playing a role similar to the aggregation-prone state. Hence, if the previously formed trimer could not achieve the most stable conformation, then by adding an additional monomer, they would require the reorganization of conformation in order to achieve a more "aggregtaion-prone conformation. As the number of strand increases in an oligomer, the need for this "stable conformation for each monomer unit will increase to stabilize the increased number of inter-strand interactions. Consequently the free energy of an oligomer is expected to decrease as the number of strands increases. In spite of obvious limitations for our simulations, their results provide useful insights for salient features of the peptide aggregation mechanism.

Concluding Remarks

We have performed replica-exchange molecular dynamics (REMD) simulations on trimer and tetramer formations of fibril-forming segments of α-Synuclein (residues 71-82) using an implicit solvation model and an all atom AMBER parm96 force field. We observed the spontaneous formation of both trimers and tetramers, demonstrating the self-aggregating and fibril forming properties of the peptides. Secondary structure profile and clustering analysis showed that oligomers with antiparallel β-sheet conformations, stabilized by well-defined hydrogen bonding, are major species corresponding to the global free energy minimum. Parallel conformations are rarely observed due to the relative instability of the parallel arrangements, which arise from the repulsive interactions between bulky and polar side chains as well as weaker backbone hydrogen bonds. Examination of free energy surfaces in relation to distances between strands indicates that the aggregation processes follow the general dock-and-lock mechanism. The time evolutions of toplogy of the free energy surface and distribution of order parameters suggest that the trimer formation process has no transition barrier, whereas the tetramer formation process has a transition barrier.

Acknowledgments. This work was supported by the National Research Foundation of Korea (NRF) grants funded

by the Korea government (MEST) (No. 2011-0000135 and No. 2010-0001630). This work is also supported by the grants (No. KSC-2009-S03-0010) and the Supercomputing Application Support Program of the KISTI Supercomputing Center.

References

1. Dobson, C. M. *Nature* **2003**, *426*, 884.
2. Ross, C. A.; Poirier, M. A. *Nat. Med.* **2004**, *10 Suppl.*, S10.
3. Skovronsky, D. M.; Lee, V. M. Y.; Trojanowskiz, J. Q. *Annu. Rev. Pathol-Mech.* **2006**, *1*, 151.
4. Chiti, F.; Dobson, C. M. *Annu. Rev. Biochem.* **2006**, *75*, 333.
5. Vilar, M.; Chou, H. T.; Luhrs, T.; Maji, S. K.; Riek-Loher, D.; Verel, R.; Manning, G.; Stahlberg, H.; Riek, R. *P. Nat'l Acad. Sci. USA* **2008**, *105*, 8637.
6. Eisenberg, D.; Nelson, R.; Sawaya, M. R.; Balbirnie, M.; Sambashivan, S.; Ivanova, M. I.; Madsen, A. O.; Riekel, C. *Accounts Chem. Res.* **2006**, *39*, 568.
7. Suk, J. E.; Lokappa, S. B.; Ulmer, T. S. *Biochemistry* **2010**, *49*, 1533.
8. Fink, A. L. *Accounts Chem. Res.* **2006**, *39*, 628.
9. Uversky, V. N.; Oldfield, C. J.; Dunker, A. K. *Annu. Rev. Biophys.* **2008**, *37*, 215.
10. Dunker, A. K.; Lawson, J. D.; Brown, C. J.; Williams, R. M.; Romero, P.; Oh, J. S.; Oldfield, C. J.; Campen, A. M.; Ratliff, C. R.; Hipps, K. W.; Ausio, J.; Nissen, M. S.; Reeves, R.; Kang, C. H.; Kissinger, C. R.; Bailey, R. W.; Griswold, M. D.; Chiu, M.; Garner, E. C.; Obradovic, Z. *J. Mol. Graph. Model.* **2001**, *19*, 26.
11. Uversky, V. N. *Protein Sci.* **2002**, *11*, 739.
12. Lucking, C. B.; Brice, A. *Cell. Mol. Life Sci.* **2000**, *57*, 1894.
13. Spillantini, M. G.; Schmidt, M. L.; Lee, V. M.; Trojanowski, J. Q.; Jakes, R.; Goedert, M. *Nature* **1997**, *388*, 839.
14. Shults, C. W. *P. Nat'l. Acad. Sci. U S A* **2006**, *103*, 1661.
15. Kim, S.; Seo, J. H.; Suh, Y. H. *Parkinsonism Relat. D.* **2004**, *10 Suppl 1*, S9.
16. Eliezer, D.; Kutluay, E.; Bussell, R.; Browne, G. *J. Mol. Biol.* **2001**, *307*, 1061.
17. Uversky, V. N.; Li, J.; Fink, A. L. *J. Biol. Chem.* **2001**, *276*, 10737.
18. Uversky, V. N. *J. Biomol. Struct. Dyn.* **2003**, *21*, 211.
19. Lee, J. H.; Lee, I. H.; Choe, Y. J.; Kang, S.; Kim, H. Y.; Gai, W. P.; Hahn, J. S.; Paik, S. R. *Biochem. J.* **2009**, *418*, 311.
20. Ulmer, T. S.; Bax, A.; Cole, N. B.; Nussbaum, R. L. *J. Biol. Chem.* **2005**, *280*, 9595.
21. Iwai, A.; Masliah, E.; Yoshimoto, M.; Ge, N.; Flanagan, L.; de Silva, H. A.; Kittel, A.; Saitoh, T. *Neuron* **1995**, *14*, 467.
22. Ma, B.; Nussinov, R. *Curr. Opin. Chem. Biol.* **2006**, *10*, 445.
23. Teplow, D. B.; Lazo, N. D.; Bitan, G.; Bernstein, S.; Wyttenbach, T.; Bowers, M. T.; Baumketner, A.; Shea, J. E.; Urbanc, B.; Cruz, L.; Borreguero, J.; Stanley, H. E. *Accounts Chem. Res.* **2006**, *39*, 635.
24. Giasson, B. I.; Murray, I. V. J.; Trojanowski, J. Q.; Lee, V. M. Y. *J. Biol. Chem.* **2001**, *276*, 2380.
25. Pawar, A. P.; Dubay, K. F.; Zurdo, J.; Chiti, F.; Vendruscolo, M.; Dobson, C. M. *J. Mol. Biol.* **2005**, *350*, 379.
26. Yoon, J.; Jang, S.; Lee, K.; Shin, S. *B. Korean Chem. Soc.* **2009**, *30*, 1845.
27. Caceres, R. A.; Timmers, L. F. S. M.; Pauli, I.; Gava, L. M.; Ducati, R. G.; Basso, L. A.; Santos, D. S.; de Azevedo, W. F. *J. Struct. Biol.* **2010**, *169*, 379.
28. Sugita, Y.; Okamoto, Y. *Chem. Phys. Lett.* **1999**, *314*, 141.
29. Case, D. A.; Cheatham, T. E.; Darden, T.; Gohlke, H.; Luo, R.; Merz, K. M.; Onufriev, A.; Simmerling, C.; Wang, B.; Woods, R. J. *J. Comput. Chem.* **2005**, *26*, 1668.
30. Onufriev, A.; Bashford, D.; Case, D. A. *Proteins* **2004**, *55*, 383.
31. Shell, M. S.; Ritterson, R.; Dill, K. A. *J. Phys. Chem. B* **2008**, *112*, 6878.
32. Ryckaert, A.; Ciccotti, G.; Berendsen, H. J. C. *J. Comput. Phys.* **1977**, *23*, 327.
33. Zhang, W.; Wu, C.; Duan Y. *J. Chem. Phys.* **2005**, *123*, 154105.
34. Nguyen, P. H.; Li, M. S.; Stock, G.; Straub, J. E.; Thirumalai, D. *P. Nat'l. Acad. Sci. U S A* **2007**, *104*, 111.
35. Thirumalai, D.; Klimov, D. K.; Dima, R. I. *Curr. Opin. Struc. Biol.* **2003**, *13*, 146.